

**STUDIES ON EFFECT OF LASER-WOOD INTERACTIONS OF
SOME MALAYSIAN HARD WOODS**

by

NOR FADHLIN BINTI JAAFAR

**Thesis submitted in fulfillment of the requirements for the
Degree of Master of Science**

December 2007

To very special people in my life:
My beloved father Jaafar bin Kassim,
My beloved mother Norkiah binti Ibrahím,
My sister Nor Jannah binti Jaafar,
My brother in law Zakri bin Md Zain,
my younger brothers Mohd Najib bin Jaafar, Mohd Najmi bin Jaafar
and
my nephews Muhammad Mukhlis, Nuruddin Fathi and Anwar Fikri

ACKNOWLEDGEMENTS

Alhamdulillah, thanks Almighty Allah for his blessings and guidance in my life. It is my pleasure to thank both of my supervisors; Assoc. Prof. Mohamad Suhaimi Jaafar and Dr. Khalid M. Omar for their constant encouragement and comments since my first step started on experiment work until the last step on thesis preparation. My deepest thank to lab assistants of both laboratories, Medical Physics and Biophysics: Mr. Yahaya and Mr. Azmi Omar. As well as technical support from Mr. Hashim and Mr. Samsudin at Machine Workshop for helping me to cut the hardwood samples and giving an idea for solution of the sample holder, my supportive families members especially my parents: Jaafar bin Kassim and Norkiah binti Iberahim that always motivate me to stay focus in my research and pray for my success and finally my post graduate friends: Izyani Karudin, Azrul Nizam Alias, Mohd Fairuz Affandi Aziz, Siti Aishah Ar. Azmi, Wan Salwani Jaafar and Rini Safitri for giving brilliant ideas and solving all the obstacles together. The journey while doing this research is very challenging and needs lots of patience, but with all motivations in myself and peoples around makes it to be a reality for completing this research. Thank you very much again.

TABLE OF CONTENTS

	Page
Acknowledgements	ii
Table of Contents	iii
List of Tables	vi
List of Figures	vii
List of Abbreviations	xiv
List of Symbols	xvi
List of Publications and Conference	xvii
Abstrak	xviii
Abstract	xix
CHAPTER 1 – INTRODUCTION	1
1.1 Laser history	2
1.2 Objectives	3
1.3 Thesis Outline	3
CHAPTER 2 - LITERATURE REVIEW	5
CHAPTER 3 - INTERACTIONS OF CO₂ LASER WITH MALAYSIAN WOODS	11
3.1 Theory of laser	11
3.1.1 Basic principles of operation	11
3.1.2 Detection of CO ₂ Laser Beam	15
3.1.3 CO ₂ laser safety	16
3.1.4 Applications of CO ₂ laser	17
3.2 Malaysian woods samples	20
3.2.1 Histology of wood	20
3.2.2 Malaysian wood specifications	25
3.3 Interactions between CO ₂ laser and woods	30
3.4 Principles of ultrasound	33
3.4.1 Principles of ultrasound	33
3.4.2 Ultrasound imaging	34

3.5	X-rays	35
3.5.1	Introduction	35
3.5.2	X-ray tube	35
3.5.3	Interaction of x-rays with matter	38
3.5.4	Object location and magnification	40
3.6	Scanning electron microscope	41
3.6.1	Development	41
3.6.2	Obtaining a signal in the SEM	42
CHAPTER 4 - RESEARCH METHODOLOGY		46
4.1	CO ₂ laser	46
4.1.1	Physical Features	46
4.1.2	Technology Overview	46
4.1.3	Cooling system	47
4.2	Laser controller	48
4.2.1	Control panel	48
4.2.2	Rear panel	49
4.3	Power meter operation	50
4.4	Ultrasound scanner	51
4.5	X-ray machine	52
4.6	Scanning electron microscope (SEM)	53
4.7	Other equipments	54
4.8	Wood samples preparation	55
4.9	Lasing process	56
4.10	X-ray technique	58
4.11	Ultrasound technique	60
CHAPTER 5 - RESULTS AND DISCUSSION		61
5.1	Comparison of surface diameter and depth penetration between two different densities of wood samples	66
5.1.1	Balau (<i>Shorea Collina Spp.</i>) and gerutu (<i>Parashorea Sp.</i>)	70
5.1.2	Kempas (<i>Koompassia malaccensis</i>) and kekatong (<i>Cynometra malaccensis</i>)	73

5.1.3	Keledang (<i>Artocarpus lanceifolius</i>) and jati (<i>Tectona grandis</i> Linn f.)	77
5.1.4	Kelat (<i>E. chlorantha</i>) and nyatoh (<i>Palaquium xanthochymum</i>)	81
5.2	Correlation between surface diameter and depth penetration with power density of two different densities of wood samples	86
5.2.1	Balau (<i>Shorea Collina</i> Spp.) and gerutu (<i>Parashorea</i> Sp.)	86
5.2.2	Kempas (<i>Koompassia malaccensis</i>) and kekatong (<i>Cynometra malaccensis</i>)	88
5.2.3	Keledang (<i>Artocarpus lanceifolius</i>) and jati (<i>Tectona grandis</i> Linn f.)	91
5.2.4	Kelat (<i>E. chlorantha</i>) and nyatoh (<i>Palaquium xanthochymum</i>)	93
5.3	Elements in exposed and unexposed region using scanning electron microscope (SEM)	97
CHAPTER 6 - CONCLUSION AND FURTHER WORK		106
6.1	Conclusion	106
6.2	Suggestions for further research	107
REFERENCES		108
APPENDICES		

LIST OF TABLES

	Page	
Table 3.1	Cutting data for various materials using carbon dioxide laser	19
Table 3.2	Malaysian Woods Specifications (according to MGR edition 1984)	29
Table 4.1	Exposure setting for hardwood samples	58
Table 5.1	Characteristic of kelat (<i>E. chlorantha</i>) and nyatoh (<i>Palaquium xanthochymum</i>)	86
Table 5.2	Elements in four hardwoods exposed regions.	101
Table 5.3	Elements in four hardwoods unexposed regions	105

LIST OF FIGURES

	Page	
Figure 3.1	Sealed CO ₂ laser construction	12
Figure 3.2	Molecular carbon dioxide modes	13
Figure 3.3	Energy states of the CO ₂ molecule	14
Figure 3.4	Classifications of parenchyma arrangements around hardwood pores (cross-section view)	21
Figure 3.5	Part of a large calcium deposit ("stone") taken from a log of Iroko (<i>Chlorophora excelsa</i>). The coin measures one inch (2.5 cm) in diameter	22
Figure 3.6	Three-dimensional orientation of wood material	24
Figure 3.7	Primary layers of wood tissue through the diameter of a tree	25
Figure 3.8	Three-dimensional of cell level comparison between hardwood and softwoods	28
Figure 3.9	Cross-section of a typical x-ray tube	36
Figure 3.10	Energy exchanges within an x-ray tube	37
Figure 3.11	Photons entering the human body will either penetrate, be absorbed, or produce scattered radiation	38
Figure 3.12	The two basic interactions between photons and electrons	39
Figure 3.13	Distance relationships in radiographic imaging	41
Figure 3.14	SEM setup	43
Figure 3.15	Scattered electron in the specimen	43
Figure 3.16	Secondary electrons (SE) and backscattered electrons (BE) regions	44
Figure 4.1	48-1 physical features of Synrad series 48-1 CO ₂ laser	46
Figure 4.2	Beam characteristics	47
Figure 4.3	Cooling system position from top view	47
Figure 4.4	Control panel	48
Figure 4.5	Rear panel	49
Figure 4.6	Target absorption versus wavelength	51
Figure 4.7	Ultrasound setup	52
Figure 4.8	X-ray machine model KXO-15R	52
Figure 4.9	Control console of x-ray machine model KXO-15R	53
Figure 4.10	SEM	53
Figure 4.11	Experimental setup for wood samples	56

Figure 4.12	Angle position setup for lasing process	57
Figure 4.13	<i>Shorea Collina Spp.</i> (balau) with holes after lasing process	57
Figure 4.14	Goggle	57
Figure 4.15	Geometrical arrangement of x-ray radiographic technique	59
Figure 4.16	Arrangements of the wood samples (top view)	59
Figure 5.1	Power of laser versus distance of laser source from wood samples at 30 seconds of laser exposure	61
Figure 5.2	Power of laser versus distance of laser source from wood samples at 60 seconds of laser exposure	62
Figure 5.3	Power of laser versus distance of laser source from wood samples at 90 seconds of laser exposure	62
Figure 5.4	Power of laser versus time of laser exposure at wood samples distance of 10 cm away from laser source	63
Figure 5.5	Power of laser versus time of laser exposure at wood samples distance of 40 cm away from laser source	63
Figure 5.6	Power of laser versus time of laser exposure at wood samples distance of 60 cm away from laser source	64
Figure 5.7	Power of laser versus PWM at 30 seconds of laser exposure	64
Figure 5.8	Power of laser versus PWM at 60 seconds of laser exposure	65
Figure 5.9	Power of laser versus PWM at 90 seconds of laser exposure	65
Figure 5.10	Surface diameter of charred wood versus time for Balau (<i>Shorea Collina Spp.</i>) at laser incident angle of 0° and PWM setting of 30% and distance between laser source and wood samples at 10 cm and 20 cm	68
Figure 5.11	Depth penetration of charred wood versus time for Balau (<i>Shorea Collina Spp.</i>) at laser incident angle of 0° and PWM setting of 30% and distance between laser source and wood samples at 10 cm and 20 cm	68
Figure 5.12	Surface diameter of charred wood versus time of laser exposure for Balau (<i>Shorea Collina Spp.</i>) at laser incident angle of 0° at 10 cm from laser source	69
Figure 5.13	Depth penetration of charred wood versus time of laser exposure for Balau (<i>Shorea Collina Spp.</i>) at laser incident angle of 0° at 10 cm from laser source	69

Figure 5.14	Surface diameter of charred wood versus laser incident angles for Balau (<i>Shorea Collina Spp.</i>) and Gerutu (<i>Parashorea Sp.</i>) for 9 and 10 minutes of laser exposures	71
Figure 5.15	Depth penetration of charred wood versus laser incident angles for Balau (<i>Shorea Collina Spp.</i>) and Gerutu (<i>Parashorea Sp.</i>) for 9 and 10 minutes of laser exposures	71
Figure 5.16	Surface diameter of charred wood versus laser incident angles for Balau (<i>Shorea Collina Spp.</i>) and Gerutu (<i>Parashorea Sp.</i>) for 11 and 12 minutes of laser exposures	72
Figure 5.17	Depth penetration of charred wood versus laser incident angles for Balau (<i>Shorea Collina Spp.</i>) and Gerutu (<i>Parashorea Sp.</i>) for 11 and 12 minutes Of laser exposures	72
Figure 5.18	Surface diameter of charred wood versus PWM for Kempas (<i>Koompassia malaccensis</i>) and Kekatong (<i>Cynometra malaccensis</i>) at 10 cm and 20 cm from laser source	74
Figure 5.19	Surface diameter of charred wood versus PWM for Kempas (<i>Koompassia malaccensis</i>) and Kekatong (<i>Cynometra malaccensis</i>) at 30 cm and 40 cm from laser source	74
Figure 5.20	Depth penetration of charred wood versus PWM for Kempas (<i>Koompassia malaccensis</i>) and Kekatong (<i>Cynometra malaccensis</i>) at 10 cm and 20 cm from laser source	76
Figure 5.21	Depth penetration of charred wood versus PWM for Kempas (<i>Koompassia malaccensis</i>) and Kekatong (<i>Cynometra malaccensis</i>) at 30 cm and 40 cm from laser source	76
Figure 5.22	Surface diameter of charred wood versus distance of laser source from wood samples for Keledang (<i>Artocarpus lanceifolius</i>) and Jati (<i>Tectona grandis Linn f.</i>) at 3 and 4 minutes of laser exposures	78

Figure 5.23	Depth penetration of charred wood versus distance of laser source from wood samples for Keledang (<i>Artocarpus lanceifolius</i>) and Jati (<i>Tectona grandis</i> Linn f.) at 3 and 4 minutes of laser exposures	79
Figure 5.24	Surface diameter of charred wood versus distance of laser source from wood samples for Keledang (<i>Artocarpus lanceifolius</i>) and Jati (<i>Tectona grandis</i> Linn f.) at 4 and 5 minutes of laser exposures	79
Figure 5.25	Depth penetration of charred wood versus distance of laser source from wood samples for Keledang (<i>Artocarpus lanceifolius</i>) and Jati (<i>Tectona grandis</i> Linn f.) at 4 and 5 minutes of laser exposures	80
Figure 5.26	Surface diameter of charred wood versus distance of laser source from wood samples for Keledang (<i>Artocarpus lanceifolius</i>) and Jati (<i>Tectona grandis</i> Linn f.) at 5 and 6 minutes of laser exposures	80
Figure 5.27	Depth penetration of charred wood versus distance of laser source from wood samples for Keledang (<i>Artocarpus lanceifolius</i>) and Jati (<i>Tectona grandis</i> Linn f.) at 5 and 6 minutes of laser exposures	81
Figure 5.28	Surface diameter of charred wood versus time of laser exposure for Kelat (<i>E. chlorantha</i>) and Nyatoh (<i>Palaquium xanthochymum</i>) at 10 cm and 20 cm from laser source	83
Figure 5.29	Depth penetration of charred wood versus time of laser exposure for Kelat (<i>E. chlorantha</i>) and Nyatoh (<i>Palaquium xanthochymum</i>) at 10 cm and 20 cm from laser source	83
Figure 5.30	Surface diameter versus time for Kelat (<i>E. chlorantha</i>) and Nyatoh (<i>Palaquium xanthochymum</i>) at 20 cm and 30 cm from laser source	84
Figure 5.31	Depth penetration of charred wood versus time of laser exposure for Kelat (<i>E. chlorantha</i>) and Nyatoh (<i>Palaquium xanthochymum</i>) at 20 cm and 30 cm from laser source	84

Figure 5.32	Surface diameter of charred wood versus time of laser exposure for Kelat (<i>E. chlorantha</i>) and Nyatoh (<i>Palaquium xanthochymum</i>) at 30 cm and 40 cm from laser source	85
Figure 5.33	Depth penetration of charred wood versus time of laser exposure for Kelat (<i>E. chlorantha</i>) and Nyatoh (<i>Palaquium xanthochymum</i>) at 30 cm and 40 cm from laser source	85
Figure 5.34	Surface diameter of charred wood versus power density for Balau (<i>Shorea Collina Spp.</i>) and Gerutu (<i>Parashorea Sp.</i>) for 9 to 12 minute of exposures	86
Figure 5.35	Depth penetration of charred wood versus power density for Balau (<i>Shorea Collina Spp.</i>) and Gerutu (<i>Parashorea Sp.</i>) for 9 to 12 minutes of exposures	87
Figure 5.36	Surface diameter of charred wood versus power density for Balau (<i>Shorea Collina Spp.</i>) and Gerutu (<i>Parashorea Sp.</i>) for laser beam angle of 0° to 50°	87
Figure 5.37	Depth penetration of charred wood versus power density for Balau (<i>Shorea Collina Spp.</i>) and Gerutu (<i>Parashorea Sp.</i>) for laser beam angle of 0° to 50°	88
Figure 5.38	Surface diameter of charred wood versus power density for Kempas (<i>Koompassia malaccensis</i>) and Kekatong (<i>Cynometra malaccensis</i>) at distances of 10 cm to 40 cm from laser source	89
Figure 5.39	Depth penetration of charred wood versus power density for Kempas (<i>Koompassia malaccensis</i>) and Kekatong (<i>Cynometra malaccensis</i>) at distances of 10 cm to 40 cm from laser source	89
Figure 5.40	Surface diameter of charred wood versus power density for Kempas (<i>Koompassia malaccensis</i>) and Kekatong (<i>Cynometra malaccensis</i>) for PWM at 40% to 70%	90
Figure 5.41	Depth penetration of charred wood versus power density for Kempas (<i>Koompassia malaccensis</i>) and Kekatong (<i>Cynometra malaccensis</i>) for PWM at 40% to 70%	90

Figure 5.42	Surface diameter of charred wood versus power density for Keledang (<i>Artocarpus lanceifolius</i>) and Jati (<i>Tectona grandis</i> Linn f.) at distances of 10 cm to 40 cm from laser source	91
Figure 5.43	Depth penetration of charred wood versus power density for Keledang (<i>Artocarpus lanceifolius</i>) and Jati (<i>Tectona grandis</i> Linn f.) at distances of 10 cm to 40 cm from laser source	92
Figure 5.44	Surface diameter of charred wood versus power density for Keledang (<i>Artocarpus lanceifolius</i>) and Jati (<i>Tectona grandis</i> Linn f.) at 3 to 6 minutes of laser exposures	92
Figure 5.45	Depth penetration of charred wood versus power density for Keledang (<i>Artocarpus lanceifolius</i>) and Jati (<i>Tectona grandis</i> Linn f.) at 3 to 6 minutes of laser exposures	93
Figure 5.46	Surface diameter of charred wood versus power density for Kelat (<i>E. chlorantha</i>) and Nyatoh (<i>Palaquium xanthochymum</i>) at distances of 10 cm to 40 cm from laser source	94
Figure 5.47	Depth penetration of charred wood versus power density for Kelat (<i>E. chlorantha</i>) and Nyatoh (<i>Palaquium xanthochymum</i>) at distances of 10 cm to 40 cm from laser source	94
Figure 5.48	Surface diameter of charred wood versus power density for Kelat (<i>E. chlorantha</i>) and Nyatoh (<i>Palaquium xanthochymum</i>) at 4 to 7 minutes of laser exposures	95
Figure 5.49	Depth penetration of charred wood versus power density for Kelat (<i>E. chlorantha</i>) and Nyatoh (<i>Palaquium xanthochymum</i>) at 4 to 7 minutes of laser exposures	95
Figure 5.50	Cross-section of an exposed region of <i>Shorea Collina</i> Spp.	98
Figure 5.51	Cross-section of an exposed region of <i>Parashorea</i> Sp.	98
Figure 5.52	Cross-section of an exposed region of <i>Artocarpus lanceifolius</i>	99
Figure 5.53	Cross-section of an exposed region of <i>Tectona grandis</i> Linn f.	99
Figure 5.54	Constituent elements in exposed region cross-section of <i>Shorea Collina</i> Spp.	100

Figure 5.55	Constituent elements in exposed region cross-section of <i>Parashorea Sp.</i>	100
Figure 5.56	Constituent elements in exposed region cross-section of <i>Artocarpus lanceifolius</i>	100
Figure 5.57	Constituent elements in exposed region cross-section of <i>Tectona grandis Linn f.</i>	101
Figure 5.58	Cross-section of unexposed region of <i>Shorea Collina Spp.</i>	102
Figure 5.59	Cross-section of unexposed region of <i>Parashorea Sp.</i>	102
Figure 5.60	Cross-section of unexposed region of <i>Artocarpus lanceifolius</i>	103
Figure 5.61	Cross-section of unexposed region of <i>Tectona grandis Linn f.</i>	103
Figure 5.62	Constituent elements in unexposed region cross-section of <i>Shorea Collina Spp.</i>	104
Figure 5.63	Constituent elements in unexposed region cross-section of <i>Parashorea Sp.</i>	104
Figure 5.64	Constituent elements in unexposed region cross-section of <i>Artocarpus lanceifolius</i>	104
Figure 5.65	Constituent elements in unexposed region cross-section of <i>Tectona grandis Linn f.</i>	105

LIST OF ABBREVIATIONS

Name	Definition
Ar ⁺ laser	Argon laser
BE	Backscattered electrons
C ₅ H ₁₀ O ₅	Pentoses
C ₆ H ₁₂ O ₆	Hexoses
CO	Carbon monoxide
CO ₂ laser	Carbon dioxide laser
CRT	Cathode ray tube
CW	Continuous wave
FOD	Focal-spot-to-object distance
FRD	Focal-spot-to-receptor distance
H ₂ O	Molecule of water
HAZ	Heat affected zone
He	Helium atom
LJW	Light hardwood
MASER	Microwave Amplification by the Stimulated Emission of Radiation
MC	Moisture content
MGR	Malaysian grading rules
MHW	Medium hardwood
ML	Middle lamella
MOE	Modulus of elasticity
MOR	Modulus of rupture
N ₂	Two nitrogen atoms
Nd:YAG laser	Neodymium-YAG (yttrium-aluminum-garnet)
NHW	Heavy hardwood
NIR	Near infrared
NOR	Nano-optoelectronic research
O ₂	Two oxygen atoms
ORD	Object-to-receptor distance
PLC	Programmable logic controller
PW	Power wizard
PWM	Pulse width modulation

Name	Definition
RF	Radio frequency
SE	Secondary electrons
SEM	Scanning electron microscopy
SID	Source-to-Image Distance
TEA-CO ₂ laser	Transverse excited atmospheric-pressure carbon dioxide laser
TEM ₀₀	Gaussian spatial distribution
UC	Ultrasonic-assisted cutting
WD	Wood density
ZnSe	Zinc selenide

LIST OF SYMBOLS

Name	Definition
A	Ampere
Al	Atomic element of aluminum
C	Atomic element of carbon
Ca	Atomic element of calcium
Co	Atomic element of cobalt
E	Energy
H	BE coefficient
h	Planck's constant = 6.626×10^{-34} Js
K	Atomic element of potassium
L	Distance between two mirrors with circular apertures
O	Atomic element of oxygen
Si	Atomic element of silicon
ν	Frequency
Z	Atomic number
/	Division slash
-	Minus sign
~	Tilde
%	Percent sign
\geq	Greater than equal to
V	Voltage
Δ	SE coefficient
\pm	Plus minus sign
$^\circ$	Degree of incident angle
=	Equals sign
Θ	Beam angular divergence
Ω_0	Distance from the beam waist
$2\omega/z$	Normal full-angle beam divergence in the far field
Ω	Gaussian width (spot size)
λ	Wavelength of laser beam
λ	Lambda
$\frac{1}{2}$	Vulgar fraction one half
π	Greek small letter pi

LIST OF PUBLICATIONS AND CONFERENCE

Nor Fadhlin Jaafar, Mohamad Suhaimi Jaafar, Khalid M. Omar, 2006 "CO₂ Laser - *Shorea Collina Spp.* Wood Interaction And Its Characterization". (5th National Seminar on Medical Physics 2006)

Nor Fadhlin Jaafar, Mohamad Suhaimi Jaafar, Khalid M. Omar and Izyani Karudin, 2007. "Interactions and Characterizations of *Shorea Collina Spp.* and *Parashorea Sp.* using CO₂ laser". (Regional Annual Fundamental Science Seminar).

Izyani Karudin, Mohamad Suhaimi Jaafar, Khalid M. Omar and **Nor Fadhlin Jaafar, 2007.** "Studies on CO₂ laser – Malaysian light hardwoods (*Shorea Uliginosa, Dyera Costulata*) and Plywood Interactions using ultrasound, SEM and EDX". (Regional Annual Fundamental Science Seminar).

KAJIAN KESAN INTERAKSI LASER DAN KAYU KE ATAS BEBERAPA KAYU-KAYAN KERAS MALAYSIA

ABSTRAK

Laser CO₂ menghasilkan alur lasernya dalam cahaya inframerah dengan prinsip panjang gelombangnya antara 9.4 μm dan 10.6 μm . Dalam kajian ini, laser karbon dioksida 10.6 μm digunakan untuk hubungkaitkan antara laser CO₂ dengan beberapa kayu keras Malaysia seperti balau, gerutu, kempas, kekatong, keledang, jati, kelat dan nyatoh. Dengan pelaseran pada pelbagai modulasi lebar denyut (PWM), masa pelaseran dan jarak daripada sumber laser ke sampel kayu-kayu keras, diameter permukaan dan kedalaman penembusan lubang telah ditentukan menggunakan kaedah sinar-x dan ultrabunyi. Selain itu, elemen-elemen di dalam beberapa kayu keras yang berharga telah diperolehi melalui imbasan mikroskop elektron (SEM). Hasil menunjukkan kuasa laser berkadar langsung dengan PWM tapi tidak bergantung pada jarak dari sumber laser ke sampel kayu keras dan masa pelaseran. Bagi tujuan pemotongan yang terbaik, set untuk setiap sampel kayu keras ini juga berbeza bergantung pada ketumpatan kayu dan struktur kayu tersebut. Karbon adalah elemen terpenting dalam kayu disebabkan elemen ini menunjukkan peratusan atom yang tertinggi antara elemen-elemen lain.

STUDIES ON EFFECT OF LASER-WOOD INTERACTIONS OF SOME MALAYSIAN HARD WOODS

ABSTRACT

The CO₂ laser produces a beam of infrared light with the principal wavelength bands between 9.4 μm and 10.6 μm. In this study, 10.6 μm is used to correlate the CO₂ laser with balau, gerutu, kempas, kekatong, keledang, jati, kelat and nyatoh. By lasing at different settings of pulse width modulation (PWM), duration of laser exposures and distances from laser source to these hardwood samples, the surface diameters and depth penetrations of the burned portions of the wood is evaluated using x-ray and ultrasonic methods. Besides, elements in valuable hardwoods also been obtained by scanning microscope electron (SEM). It shows that the power of laser varied linearly with PWM and independent of distances from laser source to wood samples and duration of laser exposure. For fine cutting purpose, the settings are also different for each hardwood samples, depending on the wood density and its structure. Carbon is the main element in wood because it has the highest atomic percentage among other elements.

CHAPTER 1

INTRODUCTION

1. Introduction

Laser cutting is a popular process in most industries. Both metallic and nonmetallic materials are cut, welded, and surface treated by different power of lasers (Zhou *et. al.*, 2004).

The thermal properties determine the amount of laser power or energy required to melt and vaporize the material including heat capacity, latent heat and heat of vaporization. Pulsed operation is usually best for deep penetration processes (drilling, cutting). The concentration of energy in each pulse leads to a small percentage of energy lost through conduction into the work-piece or dissipation to the environment. Continuous power operation is used when high average power is required, especially on the heat treatments (Han *et. al.*, 2005). Generally, the mode of CO₂ laser is continuous wave (CW) while Nd:YAG laser consider as pulsed laser.

The high technique and economic interest are improved for cutting wood machining (Sinn *et. al.*, 2005). The laser is a source of energy that can be directed on desired objects by controlling power and intensity. Use of the lasers enables to cut a great variety of materials from metal to fabrics (Ondogan *et. al.*, 2005).

1.1 History of CO₂ laser

The development of the laser has been one of the great triumphs of science last four decade. The foundations were laid by Einstein in 1917 with equation

$E = hu$ where:

E = energy

h = Planck's constant = 6.626×10^{-34} Js

u = frequency

This equation proposed by Planck to describe the spectral distribution of light emitted from a black by stimulated emission. The idea for this equation is that a system of molecules or atoms could give rise to the amplification of a beam light by population inversion.

However, a system in thermal equilibrium cannot exhibit population inversion. Purcell and Pound first demonstrated population inversion between nuclear magnetic energy level in 1951. Weber gave the first public description of the idea of amplification of microwave radiation due to stimulated emission in 1952 and the first amplifier using stimulated emission within ammonia molecule was made in 1953, was called a MASER (Microwave Amplification by the Stimulated Emission of Radiation). Maser operation was soon obtained in a wide variety of different systems including ruby. The maser principle extends to include wavelength in the optical region to make an optical maser. This was achieved by T. H. Maiman at the Hughes Research Laboratory, using ruby as the active material. Then, followed by various remarkable developments of diverse lasers in many different kind of media. CO₂ laser was one of the earliest lasers invented by Kumar Patel of Bell Labs in 1964, molecular gas laser that emits radiation in the IR region of the spectrum, the most efficient IR lasers with wavelength bands centering around 9.4 and 10.6 μm and the highest power continuous wave (CW) lasers that are currently available (Hawkes *et. al.*, 1995).

1.2 Objectives

The studies on interactions between CO₂ laser and Malaysian woods is very important because there are many problems occur such as lower edge quality and problem on work piece due by using the conventional machining.

The objectives of this research are:

- a) Determine the most suitable conditions for a fine cut, according to the interaction between CO₂ laser and Malaysian hard woods.
- b) Study the correlation between the parameters, such as the time exposure, distance between the CO₂ laser and wood samples, power density and depth penetration with different incident angle.
- c) Study the differences in depth penetration for various types of Malaysian hard woods.

Laser cutting are not really popular in Malaysia due to the high cost of the laser. Hopefully, within this project, it may promote to the manufacturers to use laser technology.

1.3 Thesis Outline

The write-up of this thesis is organized in sequence. The next chapter will discuss the literature review related to similar work in this area of research. Chapter three will give the principle of CO₂ laser including the relevant mathematical equations, an introduction on the interactions of CO₂ laser with several types of Malaysian woods and also will mention the safety precautions for a better understanding of laser interactions. The principle of ultrasound, x-ray and scanning electron microscopy (SEM) will be discussed, which are used to determine the diameter and depth penetration. Malaysian

hardwoods structure and characteristic will also be described to make a comparison of the diameter and depth penetration in varieties of woods.

In chapter four, the experimental set-up is presented including the samples of data, preparations and specifications of the ultrasound imaging, x-ray and SEM that used in this work. Chapter five included the results and discussions by using appropriate graphs and the effective of different parameters. Finally, the summary of entire work will be presented in chapter six. Some suggestions for further studies will be discussed in order to ensure the direction of research in this area stays on track and well focused.

CHAPTER 2

LITERATURE REVIEW

The excimer lasers ablation process on wood surfaces using beech and pine woods have been discussed by Panzner *et. al.* (1998). The different cut orientations and was observed by a high speed camera system and optical spectroscopy on different laser systems like excimer, Nd:YAG and TEA-CO₂ lasers. Damage of the wood surface after ablation process without carbonization of the surfaces was weaker for excimer lasers and TEA-CO₂ lasers due to the absorption properties of wood. On the other hand, thermal effects like melting and carbonization of cellulose was observed.

The interaction between an intense femtosecond laser pulses and hardwood (oak, maple and beech) surfaces and the effect of moisture on the interaction process have been studied by Theberge *et. al.* (2002). This interaction leads to ionization of many electrons. The ejection of positive and negative charge uncharred powders composition is principally wood cellulose. For all these wood samples, the ratio of the average mass of positive powders over the average mass of negative powders decreased, moisture increases and more humid the wood being.

Optodynamic studies of Er:YAG laser interaction with variety of wood targets in cube shapes such as yellow pine, black pollar, silver fit, oak, tessmania and wood composite have been done by Grad *et. al.* (1998). Depth of the hole depends linearly on the number of laser pulses. Then, time delay can be used to determine the hole depth.

A texture-based ring tracing algorithm have been developed to allow region-of-interest to be selected in terms of growth ring geometry during interactive visualization of 3D log data (Tsui, 1996). To trace the curve, Fourier texture is used and the curve thickened with morphological distance transform. Accuracy of texture orientation

estimate is limited by a few factors and a single orientation estimate is not a good approximation of the block texture.

Low power CO₂ laser is used in cutting various nonmetallic materials such as plastic, wood, particle board, and rubber by using different laser power and work piece cutting speed by Zhou *et. al.* (2004). Depth of cut is varied linearly with laser power and nonlinearly with cutting speed. The results of cutting experiments have been compared with the prediction of a theoretical model that follows the same trends.

Incision properties and thermal effects of three CO₂ lasers in soft tissue are studied by Wilder-Smith *et. al.* (1995). Many variables are involved in determining the surgical characteristic of any laser such as energy density, constant/pulsed mode, pulse durations/intervals and exposure times. All these parameters should be considered to ensure predictability, parity and consistency of results.

Application of near infrared spectroscopy (NIR) to light-irradiated wood is examined by Mitsui *et. al.* (2003). Adsorbility of water in wood varied with the light-irradiated time. This method allows the detection of changes in chemical structure of wood after light-irradiation and a new coloring method of wood.

Immunological detection of wood decay using antibodies to target fungal antigens has been reported. Two types of antibodies; polyclonal and monoclonal can be produced. Antibodies have the capacity to specifically recognize, bind and neutralize certain foreign antigens, as well as antibodies can specifically quantitate fungal antibodies within a complex structure such as wood (Clausen, 1997).

A performance comparison of CO₂ and diode lasers for deep-section concrete cutting had demonstrated by Crouse *et. al.* (2004). For practical purposes, a concrete cutting technique is better to use diode laser compared to CO₂ laser. The increased cutting

rate is due to the effects of coupling efficiency and beam shape that affords a wider and more parallel kerf.

Structure has been generalized based on systemic principles of the characteristic variables of material laser processing. The three main categories are the influence factors, the process variables and the objective functions. Han *et. al.* (2005) suggested the systemic approach is useful for experimental modeling of laser processing to optimize some performance indicators of some multi-objective functions for different laser processing method.

Comparison between ultrasonic-assisted cutting (UC) of wood and with conventional cutting on two wood species, spruce and beech in dry and wet state has been done (Sinn *et. al.*, 2005). One effect of UC is to reduce cutting force and improved surface quality. Cutting force increases with density but decrease with moisture and ultrasonic vibrations amplitudes. There is linear correlation between cutting and normal force.

The appearance of all textile products has been tried to improve from clothing to home textile using laser technology. Computer-controlled laser beam are used to change the color substances on the textile surface by directing laser beams at selected wavelength and intensity onto various textile surfaces selected for application. Tensile strength of denim trousers designed with laser beam method was 10-30% greater than the manually designed ones. Besides, designing with laser enrich the aesthetic qualities of the finished product and create a positive effect on its added value and overall quality (Ondogan *et. al.*, 2005).

Research on the temperature field in laser hardening has been done (Wang *et. al.*, 2006). Hardening effect includes the surface hardness, the depth and width of hardening layer. Their value depends on temperature field distribution in the specimen resulting from the specimen surface absorbing laser energy. The sequence of laser

technological parameters influencing the hardening effect is the laser beam spot diameter, laser beam output power and laser beam moving velocity.

High power impulse YAG laser system is used for cutting, welding and perforating of super hard materials (Usov *et. al.*, 2004). It showed that presented dependence of various materials processing parameters of various materials processing parameters upon laser beam space-and-energy characteristics have approximately linear subjection, that characterizes the developed laser system as optimal for various typed of processes applied.

The features for spinning cone water film power meter for high power CO₂ lasers are fast response, large power measurement range and high measurement accuracy (Soni *et. al.*, 2007). Besides, water absorbs CO₂ laser radiation. It showed that response of power meter is linear in the measured power meter range at differing water flow rates.

Inorganic structures located in lumina (l.) cells and walls (w.) of the cells for Dunarobba, Lukow and Arkoze woods has been investigated by using three microspectral methods (electron, x-ray synchrotron-based microprobe and μ -PIXE microprobe) except for Arkoze woods not studied for the last method (Nowak *et. al.*, 2005). It showed that calcite (l.) - goethite-hematite (w.) for Dunarobba wood, pyrite (l.) - calcite (w.) for Lukow wood and goethite (l.) - silica (w.) for Arkoze wood.

Visual, resistance drilling (probing) and stress wave or ultrasound-based techniques are all used to access the condition of wood in structures. The simplest way for locating deterioration in timber structure is by visual inspection after investigate several signs of deterioration. Resistance drilling was to characterize wood properties and detect abnormal physical conditions in structural timbers and ultrasound techniques are used in decay detection in variety of wood structure (Ross *et. al.*, 2006).

Nanoindentation was one of the nanotechnology applications by hard material of specified shape (indenter) is pressed into the surface of a softer material (substrate) with a sufficient force that the softer material deforms. It can measured the mechanical properties within cell walls in particular the S2 (thickest layer) and middle lamella (ML), allowing the interaction between wood polymer components to be more directly investigated with reduced influence of the wood hierarchical structure (Moon *et. al.*, 2006).

Wood density for majority of tropical trees is still unknown (Slik, 2006). Calculated average density of known wood of 165 Indonesian genera and one species which was randomly excluded in each genus were computed. Comparison between wood density of these excluded species and average wood density values of the genera shows that it is possible to estimate species-specific wood density patterns based on combination of known species-specific wood density values and estimation derived from genus averages in Indonesian trees.

The publication from Bond and Hamner (2007) provides information to identify wood of several species common to Tennessee by using a hand-magnifying lens. To identify, prepared the wood surface by making several thin slicing cuts of cross section. Then, determine the wood sample either hardwood or softwood based on presence or absence of vessel elements and other cell types (Bond *et. al.*, 2007).

The importance of wood density (WD) in tropical forests according to Falster (2006) are influencing the mass of the stem segment and size of the load and has direct effect on growth rate, the presumed of increased strength.

There is also a reported description of microwave transmission method that he used to estimate rapidly and nondestructively correlation to strength are density, moisture content (MC) and grain direction for sawn lumber. It had shown that the microwave

system is potentially capable of providing production-line inspection of structural lumber by recording density, MC and grain direction of the material in real time (James *et. al.*, 1985).

CHAPTER 3

INTERACTIONS OF CO₂ LASER WITH WOODS

3.1 Theory of laser

3.1.1 Basic principles of operation

The carbon dioxide laser (CO₂) is a molecular gas laser that emits radiation in the infrared region of the spectrum, and the most efficient infrared lasers available. Carbon dioxide molecules are not directly excited to higher vibrational levels to initiate lasing. Along with the CO₂, the cavity also contains nitrogen and an inert gas, typically helium. In fact, the amount of nitrogen and helium in the cavity is typically five times that of the carbon dioxide (La Salle, 2006).

The filling gas within the discharge tube consists primarily of 10-20 % CO₂, 10-20 % N₂, a few percent of H₂ and the remainder of the gas mixture is He (Wikipedia, 2006). The nitrogen gas is elevated by electrical discharge to its first excited vibrational state. When this excited N₂ molecule collides with a CO₂ molecule, there is a resonant energy transfer. Lasing occurs in the CO₂ atom to rotational levels of two different excited vibrational states (one state is associated with the molecule's symmetric stretch, the other is associated with its bending). These lasing emission occur at 10.6 μm and 9.6 μm. The helium present in the cavity acts as a buffer gas.

A typical CO₂ laser cavity is constructed of a sealed glass tube containing the gaseous mixture, with mirrors at either end (Figure 3.1) (La Salle, 2006). Typically, the mirrors are made of coated silicon, molybdenum, or gold, while windows and lenses are made of either germanium or zinc selenide (Wikipedia, 2006). ZnSe is an amber colored crystal significantly denser than glass. It absorbs very little of the light that passes through it, and can be formed into lenses. By focusing the light down into a very small

spot, it becomes possible to achieve incredible power densities; some times into the millions of watts per square meter; with that much power, the surface of most materials can not dissipate heat quickly enough and the spot erupts into a small ball of plasma (Barros, 2007). Electrical discharge is prone to dissociating the CO_2 into CO and O_2 – this problem is addressed by including H_2 or H_2O vapor in the system to replenish the carbon dioxide supply. CO_2 lasers can operate in either CW or pulsed output modes, with pulses of 0.1 to 1.0 milliseconds (La Salle, 2006).

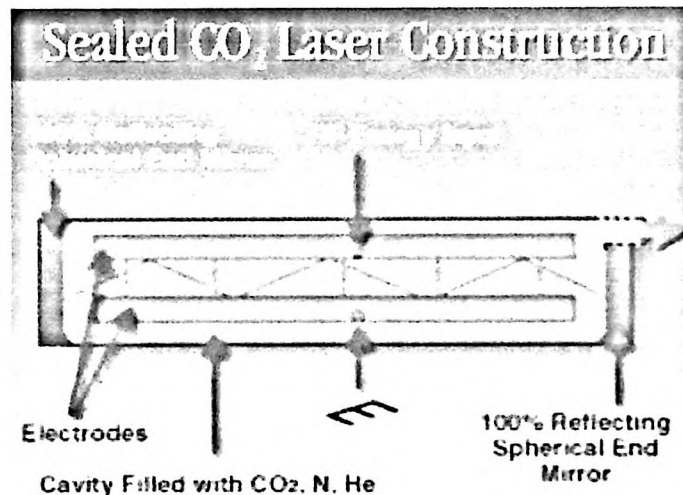


Figure 3.1: Sealed CO_2 laser construction (La Salle, 2006).

The discharge tubes normally have water jackets for cooling, for sealed-off lasers, power is not dissipated by dumping the stored energy into the flowing gas, but their heat is dissipated to the walls. Thus, water jackets are a must in order to cool the central gas and thereby avoid loss in output power (Whitehouse, 2007).

As with all lasers, in order to operate, there must be a population inversion within the lasing medium. Resonant scattering from excited nitrogen atoms causes the upper levels in the CO_2 molecules to become populated.

Of major significance to the CO_2 laser is the quantization of vibrational and rotational states of the CO_2 molecule, in addition to electronic energy levels. The CO_2 molecule

is a tri-atomic molecule consisting of 2 oxygen atoms covalently bonded to a central carbon atom (Figure 3.2) (Carpenter *et. al.*, 2007).

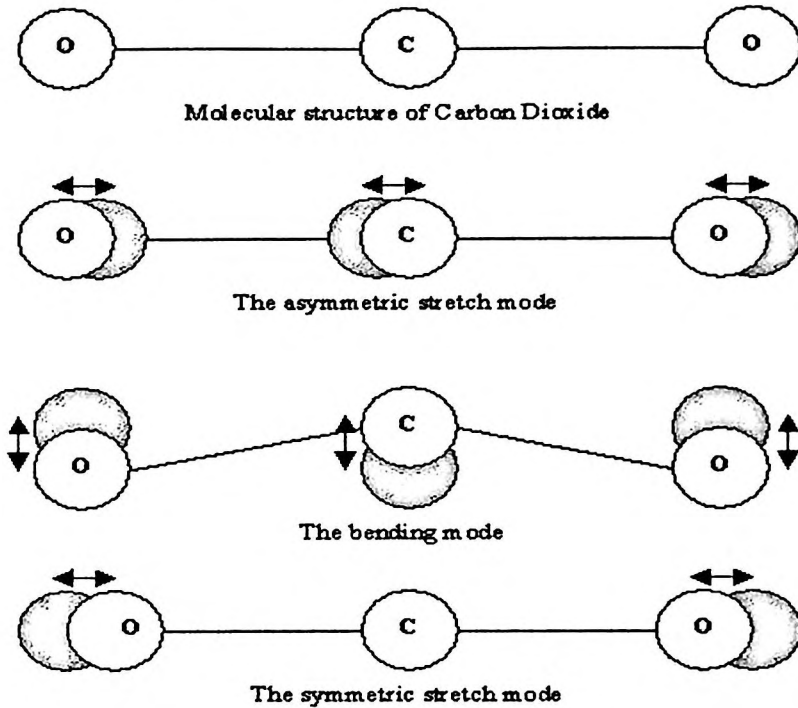


Figure 3.2: Molecular carbon dioxide modes (Carpenter *et. al.*, 2007).

In the CO₂ molecule, the individual atoms are bound by a force which acts much like that of the force due to a spring - a harmonic oscillator. Molecules vibrate due to their lacking fixed orientations within the molecule (Figure 3.2). They are able to rotate and spin because they are in a gaseous state. These states, as in electronic states, are quantized. Transitions between vibrational energy states/levels results in photon emission in the infrared, while transitions between rotational states emit photons in the microwave region. Figure 3.3 is a diagram representing some of the energy states of the CO₂ molecule.

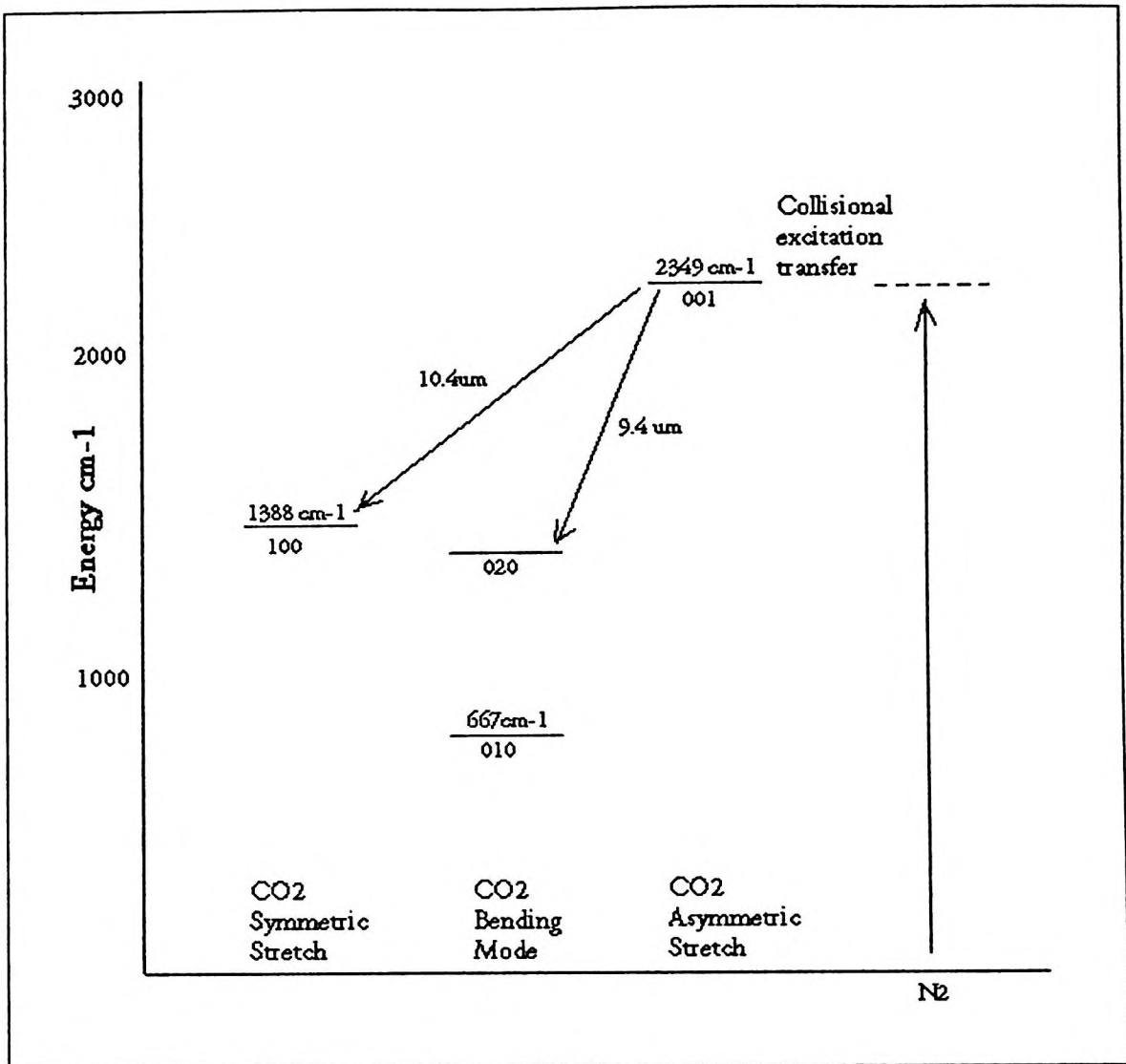


Figure 3.3: Energy states of the CO₂ molecule (Carpenter *et. al.*, 2007).

001 to 100 and 001 to 020 are the most important energy level transitions allowing emissions of 10.4 μm and 9.4 μm respectively. The 100 and 020 vibrational levels depopulate quickly. As was earlier stated, He is not only present to maintain the plasma, but also as a depopulation mechanism. When in one of these lower energy levels, a collision between CO₂ and He atoms results in a transfer of the energy to the He atom. The infrared transitions are relatively slower than this depopulation, thus a population inversion is the result. Each of the vibrational modes of CO₂ has an associated characteristic frequency of vibration (ω) along with (as can be seen above) allowed energy levels (Carpenter *et. al.*, 2007).

3.1.2 Detection of CO₂ laser beam

The most characteristics properties of laser beam are monochromaticity, coherence (spatial and temporal), directionality and brightness (Svelto, 1976). The principal purpose of a focused laser beam is to increase the intensity of the beam by condensing it into small area (Muncheryan, 1975). There are several ways to find out the CO₂ laser beam is:

- a) The simplest is to use a piece of paper in the beam. The laser is turned on for an appropriate length of time, and the burn pattern tells the location of the beam. This is also quite useful for locating the focus point of a lens illuminated with a CO₂ laser.
- b) Use phosphor plates manufactured by Optical Technology. When the 10.6 micron CO₂ laser light strikes the plate, the phosphor is deactivated. So the position of the beam appears as a dark spot on a glowing plate. Phosphor plates of different sensitivity are available.

To use a co-axial red alignment laser. The Synrad CO₂ laser has one of these, and it makes life much simpler when aligning systems of mirrors, etc. Zinc selenide is commonly used for CO₂ laser optics - lenses, beamsplitters, beam combiners, etc because it passes both CO₂ laser light and the red light of the alignment laser (Goldwasser, 2006).

3.1.3. CO₂ laser safety

A laser is a light source that can be dangerous to people exposed to it. When a beam of laser radiation is absorbed by living tissue, the damage caused is dependent on several things; the energy level of the radiation, the type of tissue irradiated, the wavelength of the laser radiation, and the time of exposure to the radiation (Muncheryan, 1975).

Lasers are classified by wavelength and maximum output power into the following safety classes. CO₂ laser classified in *class 4*: highly dangerous; even indirect scattering of light from the beam can lead to eye or skin damage. This generally applies to laser powers of more than 500 mW, or lasers that produce intense pulses of light.

The laser powers mentioned above are typical values; the classification is also dependent on the wavelength and on whether the laser is pulsed or continuous. Also, even a high power laser may be assigned to a low safety class if it is enclosed so that no laser radiation can leave the case and injure a person.

Two types of safety precautions should be considered in handling laser equipment: precautions against electrical shock and precautions against laser radiations (Muncheryan, 1975). Safety precautions are extremely important for even small CO₂ lasers for a variety of reasons:

- a) High power. Even the smallest CO₂ laser has an output beam power measured in many watts. This is enough to heat, melt, char, and burn common materials even if not particularly well focused. Human flesh including the front parts of the eye are just as susceptible to the 10.6 μm energy. CO₂ lasers are quite good at burning fingers and stuff.

- b) The beam is totally invisible. While the 10.6 μm wavelength can't reach the back of the eye and the retina, the eye can still be permanently damaged since the transparent tissues like the cornea and lens are quite sensitive to increases in local temperature.
- c) Water cooling. CO₂ lasers often use tap or recirculating water through a water jacket surrounding the tube. With many thousands of volts in close proximity, extra precautions must be taken as water and electricity don't mix very well (Goldwasser, 2006).

3.1.4 Applications of CO₂ laser

The first laser cuts were made in 1967, as part of a spin off of a military research project focused on lasers. Because the beams used in cutting are "class 4" lasers, the machines are designed to ensure that human operators are never exposed to them directly. All the cutting is done inside the machine.

Laser cutting is a way to cut precise patterns in metal, plastic, wood, and practically every other material. It allows a level of accuracy and complexity impossible with conventional machining tools. Laser cutting works by exciting a gaseous medium, commonly carbon dioxide, causing it to amplify light reflected back and forth multiple times within the laser chamber. The light emerges from an aperture and is focused by a lens onto a specific point.

Due to lasers become less focused and lose energy as they penetrate through a material, there is a limit of about 20 mm for the deepness of the cut. Moreover, a laser is made up of photons, parts of its energy can be reflected away by materials such as aluminum and copper alloys. These materials are also thermal conductors, meaning they distribute incoming heat more evenly throughout their volume. For this reason,

carbon alloy and stainless steel are popular workpiece materials for laser cutting. They are poor at absorbing heat, so heat is concentrated into the laser's path more readily (Anissimov, 2004).

There are several advantages of laser cutting such as automatic sealing of edges in synthetics, eliminate process variability due to tool wear, multilayer and kiss cutting, cutting of difficult and abrasive materials, noncontact cutting eliminates part distortion, direct integration with automated and semi-automated material handling, reduced material usage because common cut lines and reduced part margins, large cut area and fine detail from one tool, high speed, flexible pattern and perforation (Orca, 1993), no cutting lubricants required, no mechanical force on workpiece, no tool wear, very fine cut width, narrow heat affected zone and low thermal input (EBTEC, 1993).

On the other hand, laser cutting limitations are uneconomic on high volumes compared to stamping, limitations on thickness due to taper, high capital and maintenance cost and assist or cover gas required (EBTEC, 1993).

A properly controlled laser-beam radiation has many advantages over the conventional methods using in industry, and in medical and dental fields. Most of the following laser capabilities are utilized with the beam focused optically (Muncheryan, 1975).

A laser beam can weld microelectronic devices, such as transistor-package caps, transistors leads, diode leads, and similar elements, to interconnections of printed-circuit boards without causing any cracking at the weld-interface. Laser welders can weld and produce thermocouple points without creating undesirable oxidation (Muncheryan, 1975). The drilling, welding and cutting of plastics are particularly easily carried out with a CO₂ laser. The 10.6 μm radiation is highly absorbed by some plastic materials that contain absorbing compounds such as colouring dyes and their low thermal conductivity enables high local temperature to be reached quickly. The cutting

of wires and sheets of material is one of the best applications of the laser. The high speed that cuts can be made and the ease of control of laser beams facilitates numerical control. Dust and waste are reduced and the cutting operation can be almost silent (Beesley, 1976).

CO₂ lasers operating continuously can cut almost anything if the beam is focused and a jet of gas directed at the cutting area. Gas assisted is not necessary for cutting materials such as wood and paper but the use of an inert gas or carbon dioxide reduces charring by preventing the ignition of gaseous by-products in the vicinity of the cut. Inert gas jets may also be advantageous in producing clean cuts in other materials by rapidly removing by-products (Beesley, 1976).

Table 3.1 lists some examples of materials that have been successfully cut using continuous wave CO₂ laser with details of thickness, cutting rates and gas assistance (Beesley, 1976).

Table 3.1: Cutting data for various materials using carbon dioxide laser (Beesley, 1976)

Material	Thickness (mm)	Laser power (W)	Power density (MWcm ⁻²)	Gas	Cutting rate (cms ⁻¹)
Mild Steel	0.5	200	-	oxygen	1
	3	350	0.5	oxygen	1.5
Stainless Steel	0.5	200	-	oxygen	4.4
Titanium	0.6	200	-	air	0.3
	1.5	300	0.25	oxygen	4
Zirconium	0.25	200	-	air	1.5
Nimonic 90	1.5	250	0.4	oxygen	1
Sintered Carborundum	1.6	200	-	air	1.3
Asbestos Cement	6.3	200	-	air	0.04
Silica	1	600	2	none	5
Glass	4	200	-	air	0.16
Perspex	25	200	-	air	0.16
Nylon	0.8	200	-	air	8
PTFE	0.8	200	-	air	10
Leather	3.2	200	-	air	10
Deal	50	200	-	air	1.5
Oak	18	200	-	air	3
Teak	25	200	-	air	0.12
Synthetic Rubber	2.5	600	2	nitrogen + steam	4

When a laser beam is used with a proper waveguide, it can perform bloodless surgery, remove tumors from the brain cavities, and perform bloodless operations on the kidney, liver, lungs, stomach, and pancreas. It can remove tattoos from human extremities and it can drill holes, cauterize tissue, and strengthen enamel in dental work (Muncheryan, 1975). Moreover, lasers can be used as surgical knives. The infrared light of medium-power (20-100 W) CO₂ lasers (~10.6 μm) is strongly absorbed by the water contained in the tissue and results in an efficient coagulation (of small vessel). Lasers are often used in the medical field to treat cases of detached retina. Laser light aimed through the lens of the eye is focused to a number of very small spots (that obviously have to be kept sufficiently far away from the optic nerve). The laser beam "welds" the retina in position at the back of the eye. Ar⁺ lasers are most commonly used for this application (Svelto, 1976).

3.2 Malaysian woods samples

3.2.1 Histology of wood

Wood is not solid, homogeneous substance but a porous one composed of large numbers of very small elements or cells, the cavities with in the dry condition at least, are largely occupied by air. All cells of wood is composed from an outside layer known as vascular cambium.

The cells of this cambium are living cells, each consisting of a protoplast enclosed in a cell wall and are of two kinds; spindle-shaped, axially elongated cells, the fusiform initials and the ray initials which are cells about as broad s they are high. Each cell of the vascular cambium possesses a thin wall of its own, and a thin layer of intercellular substance, the middle lamella, unites adjacent cells. When a cell divides into two cells, this middle lamella is formed as primary wall and upon it the new wall of each cell is deposited. The middle lamella is composed largely of pectic materials, and the primary walls consist mainly of cellulose and pectic substances. The secondary wall, at its

inception, consists of cellulose and related compounds. Meanwhile, lignin a complex substance that chemical composition has to be fully determined (Jane, 1970).

A cell cut off from the vascular cambium, toward the wood, may differentiate into one of the four types of xylem element: parenchyma cell, fibre, tracheid or vessel element. Parenchyma cell serve for storage food reserves, as depositories for waste materials, pass on food and water to other parts of the wood and have supporting function (Jane, 1970). There are two basic types of parenchyma: *paratracheal* and *apotracheal*. The major difference between them is that paratracheal parenchyma makes contact with the pores or vessel elements, while apotracheal parenchyma is separated from pores by fibers or rays. Figure 3.4 shows the cross section of various types of paratracheal and apotracheal parenchyma. In most species, apotracheal parenchyma are not be useful in identifying wood with just a hand lens, paratracheal parenchyma appears in many forms and is often more useful in identification (Bond *et. al.*, 2007).

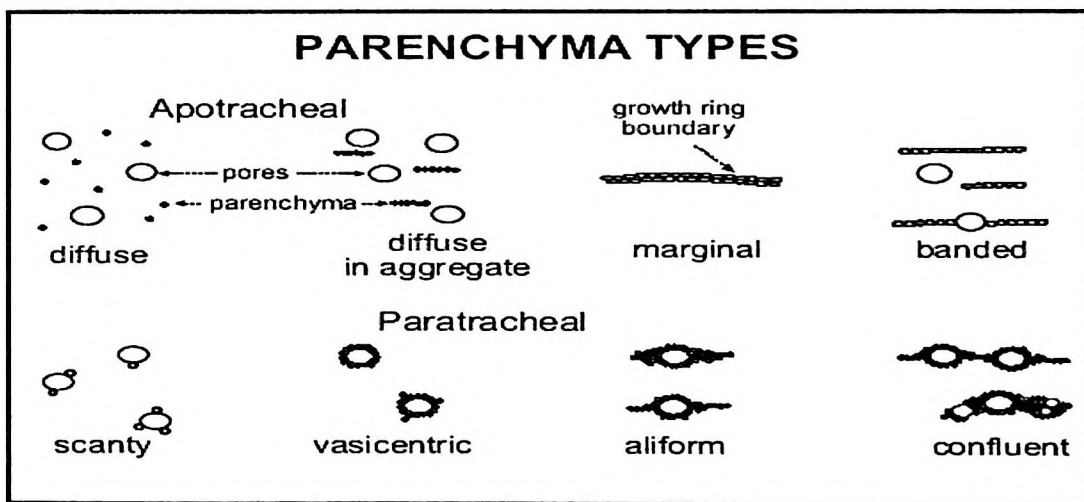


Figure 3.4: Classifications of parenchyma arrangements around hardwood pores (cross-section view) (Bond *et. al.*, 2007).

Vessels and tracheids are conducting element, serving to convey water and dissolved mineral salts from the roots to the leaves. A tyloses is an extension of a living parenchyma cell, containing protoplasm and nucleus of the parent cell that may pass

into it (Jane, 1970), form inside the vessels of some hardwoods, effectively clog the vessels and subsequently restrict moisture movement (Bond *et. al.*, 2007).

Although wood consists almost entirely of cellulose and related substances, and lignin is often contains an extractives or extraneous substances-gums, resins, tannins, oils, colouring matters, starch, latex, inorganic salts and other materials. Mineral deposits usually referred as white deposits, while any gummy material in softwood is resin, and in hardwood, a gum, although the two groups of substances are sharply distinguished. A wood is said to contain oil if it has an oily feel such as teak, although the so-called oil in this wood is aloe-resin. The inorganic materials in wood consist chiefly of silica and salts of calcium and occur mainly in the lumina of the cells (Figure 3.5) (Jane, 1970).

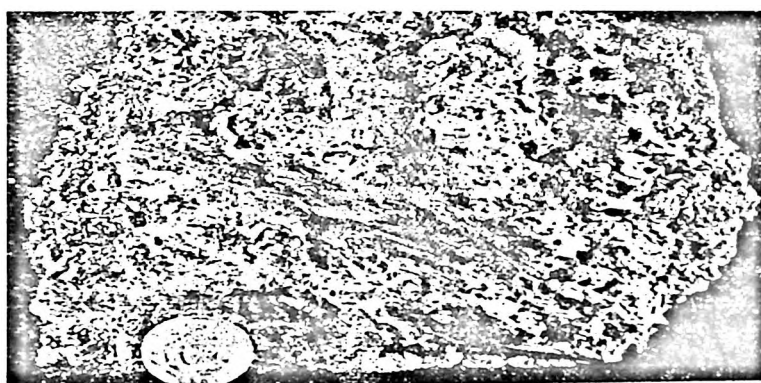


Figure 3.5 Part of a large calcium deposit ("stone") taken from a log of Iroko (*Chlorophora excelsa*). The coin measures one inch (2.5 cm) in diameter (Jane, 1970).

Starch is formed exclusively in living cells and hence in parenchyma, both axial and ray parenchyma, where it is stored as a reserve food material. Oils that less commonly occupy these cells may be stored for the same purpose. Essential oils and tannins are sometimes found in special parenchyma cells. Gums, resins and other materials of this type may occur in vessels, tracheids, parenchyma and fibres.

True gums are carbohydrate substances, soluble in water but not in alcohol, and are usually formed by the breakdown and degradation of the cell walls of the wood. The resins that are oxidation products of certain essential oils, complex substances of

varied chemical composition, insoluble in water but soluble in alcohol. Hard resins like copals and gum dammar, contain little or no essential oil. The oleo-resins contain a considerable quantity of oil and are more or less liquid. The gum resins are mixtures of true gum and resin (Jane, 1970).

The structure of wood spans many length scales: meters for describing the whole tree, centimeters for describing structures within the tree cross section (pith, heartwood, sapwood and bark), millimeters for describing growth rings (earlywood, latewood), tens of micrometers for describing the layer structure within cell walls, tens of nanometers for describing the configuration of cellulose fibrils in matrix of hemicellulose and lignin, and nanometers for describing the molecular structures of cellulose, hemicellulose and lignin and their chemical interactions. Wood cell development occurs initially with the creation of a porous cellulose-hemicellulose structure followed by an intergrowth of lignin (lignification) within this structure (Moon, 2006).

Wood is composed of many small cells and its structure is determined by the type, size, shape and arrangement of these cells. Wood surfaces are classified into three categories or geometric planes of reference that indicate the type of surface uncovered after a cut has been made. The three reference planes are the cross section, radial section and tangential section (Figure 3.6) (Bond *et. al.*, 2007).

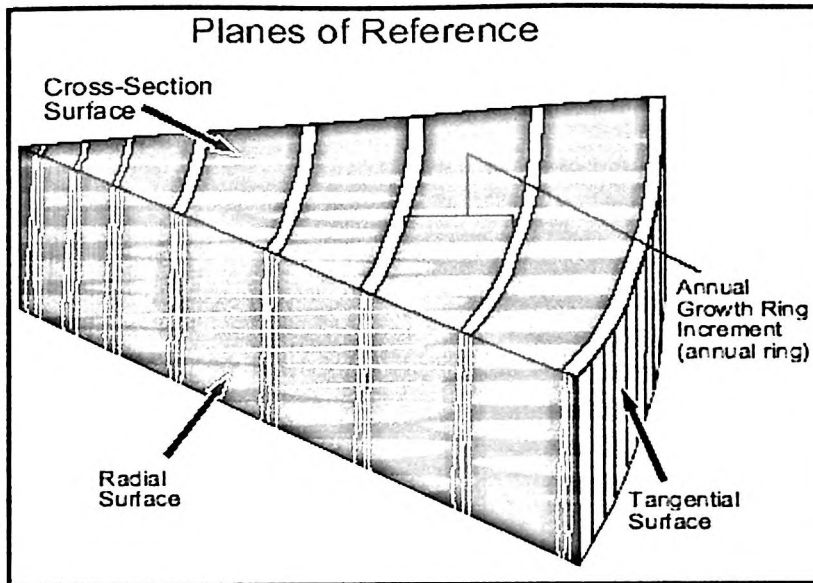


Figure 3.6: Three-dimensional orientation of wood material (Bond *et. al.*, 2007).

Cross section of the wood is produced by cutting the cells perpendicular to the direction of growth in the tree. The cross section is the same surface seen on a stump after felling a tree. By cutting a tree and exposing the cross section, you can observe the bark, phloem (bark-producing layer), cambium (a thin layer inside the bark that cell division takes place) and xylem (sapwood and heartwood) can be observed (Figure 3.7). The heart-wood is the darker-colored material that is formed in the center of the tree and contains extractives that are the chemical components. The sapwood surrounds the heartwood and is lighter-colored. The size and width of the sapwood will vary greatly between species. A growth ring represents one year of wood formation. The development of the wood material inside a growth ring is caused by the changes that occur during the growing session (Bond *et. al.*, 2007).